ELSEVIER

Biophysical Chemistry 60 (1996) 29–38

Biophysical Chemistry

Experimental model for the thermal denaturation of azurin: a kinetic study

R. Guzzi [a], C. La Rosa [b], D. Grasso [b], D. Milardi [b], L. Sportelli [a,*]

[a] *Dipartimento di Fisica, Laboratorio di Biofisica Molecolare, Università della Calabria and Unità INFM, 87036 Arcavacata di Rende, Italy*

[b] *Dipartimento di Scienze Chimiche, Università degli Studi di Catania, 96125 Catania, Italy*

Received 24 April 1995; revised 21 June 1995; accepted 17 September 1995

Abstract

The thermal denaturation of azurin in H_2O, D_2O and in ethanol–H_2O mixtures has been investigated by electron spin resonance (ESR), optical absorption spectroscopy and differential scanning calorimetry (DSC). The OD_{625}/T variation observed at a scan rate of 0.7°C/min in H_2O shows a cooperative OD transition between 78 and 82°C. In this step the intense charge-transfer band of azurin at 625 nm disappears. The ESR spectra recorded at −153°C of the protein in the native state and after heating at 80 and 82°C indicate that both the symmetry and the copper ligands change with the thermal transition. The DSC measurements show that the thermal denaturation of azurin, which occurs at 84.4°C, is irreversible and kinetically controlled. This complex transition has been described as a multistep denaturation path and was analysed using a Lumry–Eyring type mechanism. The experimental $C_{p,exc}$ profile has been simulated and the calorimetric enthalpies related to the reversible and irreversible step, ΔH_u and ΔH_{ag}, respectively, are obtained. The kinetically controlled steps have been investigated by means of optical and DSC measurements at different scan rates and the apparent activation energy, E_a, has been calculated. The denaturation of azurin in D_2O and ethanol–H_2O mixtures follows the same denaturation path as in H_2O, although a shift of the OD_{625}/T and DSC profiles is evidenced. The temperature of the thermal transition and the E_a values decrease in ethanol–H_2O mixtures, but increase in D_2O.

Keywords: Azurin; Thermal denaturation; Optical density; Differential scanning calorimetry; Solvent effect; Kinetic methods

1. Introduction

The investigation of the protein–solvent interaction has received a lot of attention because the structure–function relationship of these macromolecules strongly depends on this interaction. Since most proteins operate in aqueous solutions, the importance of water has long been recognized and deeply investigated [1]. The structure of native proteins is determined by the balance of intra- and intermolecular interactions between different amino acid residues and between these residues and the water molecules surrounding the proteins. This balance determines the tendency of individual amino acid residues to prefer either the interior or the surface of the proteins [2].

Moreover, these interactions [3,4] can change if perturbing agents such as denaturants [5–7] or stabilizers [8] are present in solution as well as by tem-

* Corresponding author. Fax: (39)-984 839389.

SSDI 0301-4622(95)00138-7

perature [9,10] and pH variations [11,12]. In this case the overall structure of the proteins is weakened or strengthened, depending on the properties of the perturbing molecules. The investigation of these changes provides valuable information about the role of the solvent in maintaining the conformation of native proteins.

Azurin is an electron-transfer bacterial protein containing a single Cu^{2+} type I center [13–15]. The three-dimensional structure of azurin can be described as an eight-stranded β-sandwich with a small α-helical flap on the outside. The geometry of the copper site is trigonal bipyramidal with one S from Cys-112, two N from His-117 and His-46 in the equatorial plane (copper is about 0.1 Å above the trigonal plane) [16–18] and two weakly bound axial, one S from Met-121 and one O from Gly-45. The cysteine sulphur in the donor set gives rise to the intense $p\pi S(Cys) \rightarrow d_{x^2-y^2}(Cu^{2+})$ charge-transfer absorption, which is primarily responsible for the absorbance at 625 nm [19,20]. The Cu^{2+} ion is bound at about 7.5 Å from the protein surface buried in a very hydrophobic pocket shielded from the solvent, although one edge of a histidine ligand is accessible to the solvent [21].

The aim of this paper is to investigate the thermal denaturation of azurin in H_2O and to look at how different solvents affect this process. The solvents used are D_2O and ethanol–water mixtures.

It has been found that the thermal denaturation of azurin in H_2O is irreversible and under kinetic control. The overall denaturation is described by a multistep denaturation path. The path remains quite unchanged in the other solvents although the optical density (OD) and differential scanning calorimetry (DSC) profiles are shifted to higher (D_2O) or lower (ethanol–H_2O mixtures) temperatures.

The results stress both the important role of the copper ion in stabilising the protein and for a marked effect of the physical-chemistry properties of the solvent on the thermal denaturation of azurin.

2. Experimental

2.1. Materials

Lyophilized azurin from *Pseudomonas Aeruginosa* was purchased from Sigma (Germany) and used without further purification. The optical density ratio OD_{625}/OD_{280} measured at room temperature was 0.44. Ethanol was from Farmitalia (Carlo Erba) and D_2O (99.9%) from Merck. A 10 mM phosphate buffer solution (PBS) at pH 7.0 prepared with salt of analytical-reagent grade was used throughout. Negligible effects on the pH were found even at the highest alcohol molar fractions used.

Protein concentration was checked spectrophotometrically at room temperature at $\lambda = 625$ nm using a molar extinction coefficient ε_{625} of 5000 M^{-1} cm^{-1}. The ethanol–water mixtures were prepared with an ethanol molar fraction, χ_f, ranging between 0 and 0.049.

2.2. Methods

2.2.1. Optical absorption

The optical absorption measurements were carried out with a Jasco 7850 spectrophotometer equipped with a Haake thermostated bath Model D8-G (± 0.1°C). Quartz cuvettes with 1 cm optical path were used throughout. The temperature of the samples was measured directly by a YSI precision thermistor dip in the reference cuvette. Azurin concentration was 4.7×10^{-5} M. The measurements were started 3 min after positioning the samples in the thermostated sample holder at the initial temperature of 50°C. The heating rates were 0.3, 0.7 and 1.0°C/min. The temperature of the optical transition, T_t, is defined as the midpoint of the OD transition.

The kinetics of the thermal denaturation of azurin were studied by following the time-dependent OD_{625} variation at temperatures $T \leq T_t$. First-order rate constants (k_1) of the thermal denaturation of azurin in H_2O, in D_2O and in ethanol–water mixtures were calculated by fitting the OD_{625}–time profiles with the following expression [22]:

$$OD_{625}(t) = OD_{625}(\infty) + [OD_{625}(0) - OD_{625}(\infty)]e^{-k_1 t} \quad (1)$$

where $OD_{625}(0)$ and $OD_{625}(\infty)$ are the optical density at $t = 0$ and $t = \infty$, respectively.

The k_1 values derived from these fittings were found to be highly temperature dependent. By means of an Arrhenius analysis of k_1 data, the apparent activation energy, E_a, values were calculated for azurin in all the solvents used.

2.2.2. Differential scanning calorimetry

DSC scans were made with a Setaram (Lyon, France) micro differential scanning calorimeter with stainless steel 1-ml sample cells interfaced with a Bull 200 Micral computer. Both the sample and the reference were scanned from 30 to 100°C with a precision of ± 0.08°C. In order to obtain the C_p curves, buffer–buffer base lines were obtained at the same scanning rate and then subtracted from sample curves. The $C_{p,exc}$ functions related to the thermal unfolding of azurin were routinely obtained by using a 4th order polynomial fit simulating the trend of C_p of native and denaturated form in the denaturation range as previously suggested [23]. The average level of noise was about 0.4 μW and the reproducibility at refilling was about 0.1 mJ/K/ml. Energy calibration was performed with an EJ2 Setaram Joule calibrator. The protein concentration used was 1.2 mg/ml

2.2.3. Far-UV circular dichroism

Circular dichroism (CD) measurements in the far-UV region were performed with a JASCO 700 spectropolarimeter using quartz cuvettes of 1 mm optical path. Azurin concentration was 0.35 mg/ml.

2.2.4. Electron spin resonance

The electron spin resonance (ESR) measurements were carried out with a Bruker ER 200D-SRC X band spectrometer equipped with the ESP 1600 data system. All the ESR spectra were recorded at -153°C, but samples had different thermal histories. A cold nitrogen flow was used to reach this temperature, which was controlled with an accuracy of ± 0.3°C by means of the ER 4111 VT (Bruker) temperature control system. The protein concentration was 1.7×10^{-4} M.

From the ESR spectra, the $g_{\parallel}$ component of the axial symmetric **g** tensor and the $A_{\parallel}$ component of the hyperfine interaction tensor **A** were extracted. These two magnetic parameters give information about the geometry and ligand atoms of the copper ion in azurin.

Finally, it is worthwhile to point out that the different experimental techniques used required a different protein concentration in order to obtain an acceptable signal-to-noise ratio. However, no concentration dependence of the experimental data has been observed.

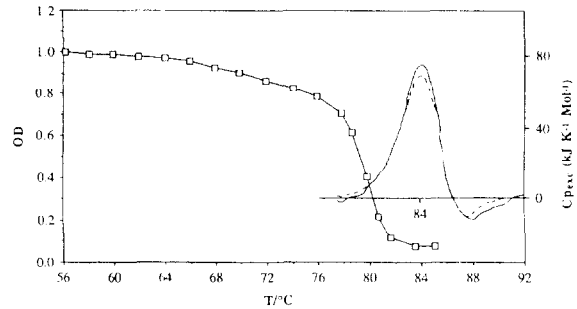

Fig. 1. Normalized OD_{625} vs. temperature variation of 4.7×10^{-5} M azurin in H_2O at a scan rate of 0.7°C/min. On the right-hand site the $C_{p,exc}$ curve is reported (solid line), obtained at a scan rate of 0.7°C/min of native azurin, and its simulation (dashed line) with Eq. 4 in the text.

3. Results and discussion

3.1. Thermal denaturation of azurin in H_2O

The active-site-bound copper is a suitable built-in probe useful for obtaining information on the copper environment during the thermal denaturation of azurin. In fact, since the copper ion is bound in the interior of the protein, any significant change in tertiary or secondary structure would be expected to alter the properties of the copper center and, in turn, the VIS absorbance.

Fig. 1 shows the optical density of the $p\pi S(Cys) \rightarrow d_{x^2-y^2}(Cu^{2+})$ charge-transfer band at $\lambda_{max} = 625$ nm vs. temperature (OD_{625}/T) of azurin in aqueous solution recorded at a scan rate of 0.7°C/min. As can be seen, OD_{625} evidences a near-linearly OD decrease up to 76°C and then a single cooperative transition in the temperature range 78–82°C with a transition temperature of $T_t = 80$°C. Upon cooling to room temperature after the OD transition at 80°C, only the Cu^{2+} $d \rightarrow d$ VIS absorption band is observed. As the disappearance of the charge transfer (CT) transition could also be due to the oxidation of the copper-coordinated cysteine at higher temperatures, the thermal denaturation has been investigated in nitrogen atmosphere too. The OD/T profile obtained (not reported) is exactly the same as recorded

in the presence of oxygen. Thus, the loss of the blue colour has to be ascribed to conformational changes of the azurin tertiary structure, which permanently alter the relative position of the copper ion ligands. Hereafter, to compare our results with those in the literature [24], all measurements were carried out under aerobic conditions.

In order to investigate how the temperature-induced copper binding site modification is related to the protein denaturation, we have performed DSC measurements on azurin in H_2O at $v = 0.7°C/min$ (Fig. 1, right-hand side). By comparing the OD_{625}/T and DSC profiles it can be noted that a significant heat absorption occurs at 84.4°C, i.e., after the OD_{625} transition. In fact, the heat absorption up to 80°C is very low, $\Delta H = 36 \pm 7$ kJ/mol. Moreover, an exothermic contribution at higher temperatures is present.

Sequential heating experiments carried out on azurin have shown that the optical and DSC detected thermal transitions are separate, irreversible processes. In fact, after the protein has been heated to 80°C (through the active site disruption) and rapidly cooled to room temperature, the CT absorption band is no longer present, but the DSC transition is still observed upon rescanning (Fig. 2). In a subsequent scan, neither transition appears. These measurements allow us to exclude that at T_t the copper ion is released. In fact, the DSC profile in Fig. 2 differs from that of apo-azurin reported by Engeseth and McMillin [24], which shows an endothermic heat absorption at 62°C, with $\Delta H = 245$ kJ/mol, and another one at 86°C, with $\Delta H = 367$ kJ/mol. In addition, no exothermic contribution at high temperatures was present in the apo-protein.

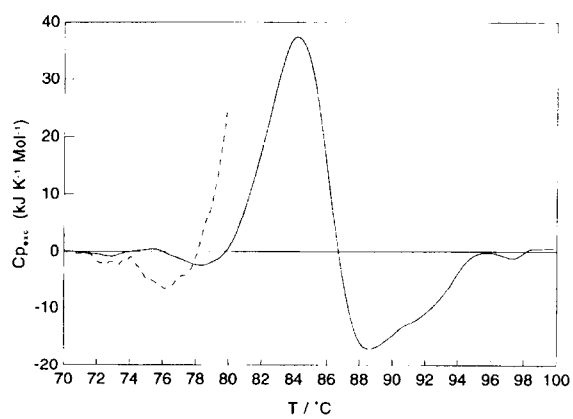

Fig. 2. DSC profile of azurin in aqueous solution up to 80°C (– – –) and rescan of the same sample after a rapid cooling to room temperature (—).

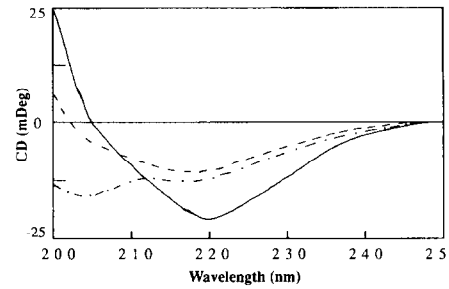

Fig. 3. Far-UV CD spectra of azurin in H_2O in the native state (—), after heating up to 80°C (– – –) and after the DSC transition (– · – · –).

Fig. 3 shows the far-UV CD spectra of azurin in the native state (solid line), after heating to 80°C (dashed line) and in the denaturated state (dashed and dotted line). These results suggest that during the first heating up to 80°C the bonds between Cu^{2+} and the ligands are weakened, together with the tertiary structure, and when the DSC transition takes place, the protein loses the secondary structure.

Temperature-induced changes in the copper coordination geometry are also evidenced by ESR spectroscopy. The measurements have been carried out at −153°C on the folded form of azurin (Fig. 4a) and on a sample which was previously heated to 80°C (Fig. 4c). Both the ESR spectra and the magnetic parameters in Table 1 indicate an irreversible alteration of the copper center after the raise in temperature. In fact, a new resonance line at 2700 G and an increase from 55 to 60 Gauss in the $A_{\parallel}$ value are evidenced in the modified form of azurin, obtained at 80°C. Negligible changes are observed in the perpendicular region of the copper signal. The ESR spectrum of azurin recorded after the OD transition (82°C) is very similar to that usually obtained for a type 2 complex with a square planar symmetry (Fig. 4d). As concerns the copper ligands, using the correlations with simple Cu^{2+} complexes [25,26] the $g_{\parallel}$ and $A_{\parallel}$ values ($g_{\parallel} = 2.284$ and $A_{\parallel} = 160$ G) suggest the presence of nitrogens and oxygens in the donor set. However, as the loss of the CT band indicates

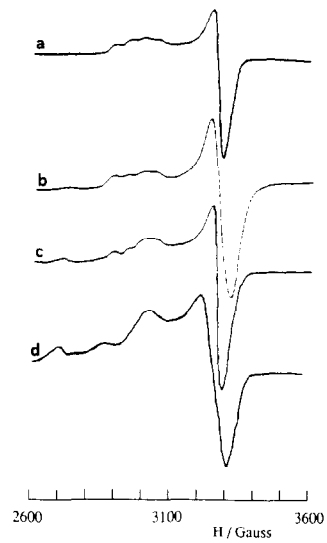

Fig. 4. Experimental ESR spectra at $T = -153$°C of 1.7×10^{-4} M azurin in aqueous solution. (a) Native azurin, (c) azurin heated at 80°C and (d) azurin heated at 82°C. In (b) the computer simulation of spectrum (c) is shown (for details see text).

only an increase in the Cu–S bond length, we cannot exclude, in principle, the presence of sulphur in the Cu coordination shell. An exact assignment should require nuclear magnetic resonance (NMR) measurements. This will be the subject of further study.

The experimental ESR spectrum at 80°C (Fig. 4c) has been simulated in terms of weighted sums of two spectra with the spectral features (Table 1) of native and colourless azurin assuming axial symmetry [18]. As can be seen, the simulation reported in Fig. 4b is excellent and suggests that at 80°C a conformational transition, which involves the copper environment, takes place. The conformational modification favours the rearrangements of the copper donor set.

Our optical, magnetic and DSC data obtained at 0.7°C/min show that: (i) from 78 to 82°C azurin changes, to some extent, the tertiary structure and the Cu–S bond length increases (OD not recovered and ESR spectrum completely changed). Moreover, the modified folded form of azurin existing in this temperature range retains the β-barrel structure as the far-UV CD spectrum in Fig. 3 shows. (ii) The subsequent endothermic phenomenon, as evidenced by DSC, induces conformational changes and loss of the secondary structure. (iii) At high temperatures, the aggregation processes (exothermic peak) of azurin polypeptide chains take place, which determine the irreversibility of the thermal denaturation.

Table 1
Magnetic parameters used for computer simulation of the native and thermally denaturated azurin to reproduce the Cu^{2+} ESR spectrum obtained by stopping the thermal denaturation process at 80°C

	$g_{\parallel}$	$g_{\perp}$	$A_{\parallel}$ (G)	$A_{\perp}$ (G)
Az (native)	2.271	2.052	55	15
Az (denaturated)	2.284	2.045	160	15

In order to rationalize the thermal denaturation of azurin, the following scheme can be put forward:

$$N \xrightarrow{k_1} N\text{–}Cu^{2+} \xrightarrow{k_{app}} F \qquad (a)$$

where N represents the native azurin, $N\text{–}Cu^{2+}$ the folded protein with altered copper center, and F the final state, while k_1 and k_{app} are the optical and the calorimetric kinetic constant of the two processes, respectively.

The first step takes into account the OD-detected transition from the native to the colourless form of azurin which occurs with $\Delta H = 36 \pm 7$ kJ/mol (Fig. 1). In this temperature range the β-barrel structure of the protein is only weakened (Fig. 2, dashed line).

In the second step, the colourless folded form of the protein, $N\text{–}Cu^{2+}$, undergoes a complex, complete and irreversible denaturation process to the final state, F. A large enthalpy change is associated with this process which gives rise to the DSC transition.

The kinetically controlled steps of reaction scheme a have been investigated by means of optical and DSC measurements at different scan rates. The OD_{625}/T and the DSC profile as a function of the scan rate are reported in Fig. 5A and B, respectively.

From the DSC profiles the apparent activation energy, E_{app}, has been calculated by means of the equation [22,27]:

$$\ln\left(\frac{v}{T_m^2}\right) = \text{const} - \frac{E_{app}}{RT_m} \qquad (2)$$

where v is the scan rate (°C/min), T_m is the temperature of the maximum heat absorption and R is the gas constant. From the $\ln(v/T_m^2)$ versus $1/T_m$ plot, an E_{app} value of 356 kJ/mol was calculated.

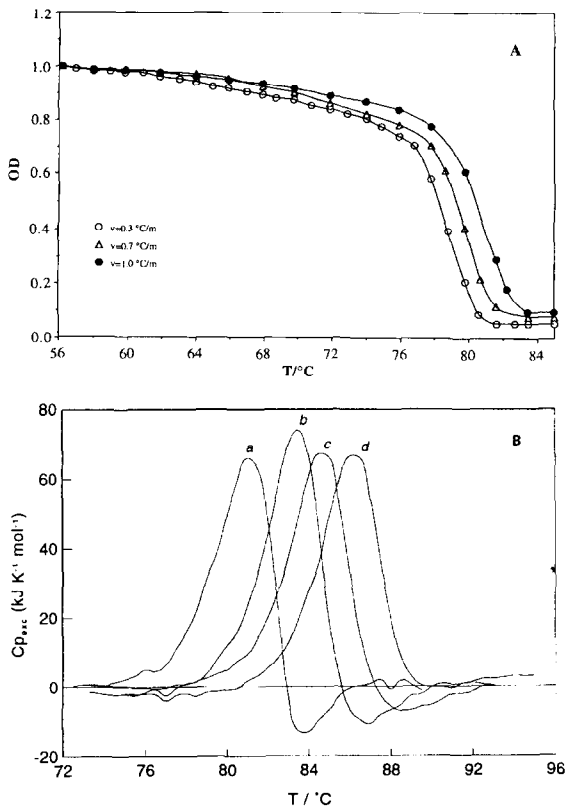

Fig. 5. (A) Normalized scan rate dependent OD_{625} vs. temperature curves and (B) DSC profiles obtained at scan rates of: (a) 0.3, (b) 0.5, (c) 0.7 and (d) 1.0°C/min.

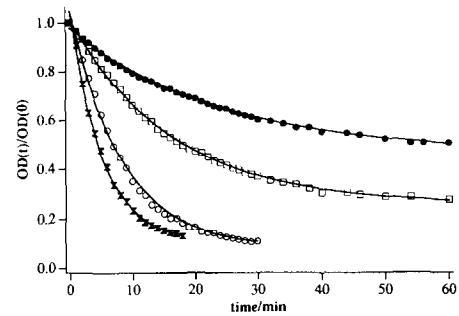

Fig. 6. Normalized OD_{625}/time decay curves of azurin in aqueous solution at (▼) 80°C, (○) 79°C, (□) 78°C and 77°C (●). The full lines represent the best fits of the experimental points according to Eq. 1.

In addition, by supposing that the process of disruption of the active site is also a first-order process and using Eq. 2 where T_m and E_{app} are now substituted by T_t and E_a (the temperature of the OD_{625}/T transition and the activation energy, respectively), we obtain $E_a = 451$ kJ/mol.

An equal E_a value can also be obtained by means of time-dependent OD variations at fixed temperatures [22]. From non-linear, least-squares fitting of Eq. 1 to the experimental points (Fig. 6), the k_1 values at 80, 79, 78 and 77°C have been calculated, and the Arrhenius equation

$$\ln k_1 = \text{const} - \frac{E_a}{RT} \qquad (3)$$

was used to calculate the activation energy. From the corresponding plot, $\ln k_1$ vs. $1/T$, a value of $E_a = 441$ kJ/mol was calculated (Table 2). This E_a value corresponds very well with that previously found using OD_{625} scan rate dependent data, but differs from that of $E_{app} = 356$ kJ/mol found by calorimetry. The origin of this difference is not surprising. The calculated apparent activation energies are related to different phenomena which concern the irreversible disruption of the native Cu^{2+}–N_2SS^*O active site of azurin and of azurin on the whole.

Since the thermal denaturation of azurin is irreversible, it cannot be analysed in thermodynamic terms. However, since the second process in reaction scheme a, i.e., $N\text{–}Cu^{2+} \rightarrow F$, is complex, a decom-

Table 2
Temperature values and thermodynamic parameters of azurin thermal denaturation in the presence of ethanol at different molar fraction, χ_f, and in D_2O as found from the OD_{625}/T measurements at a scan rate of 0.7°C/min and DSC ones at a heating rate of 0.5°C/min. The apparent activation energies, E_a, as evaluated from kinetic experiments, are also reported

OD_{625}			DSC	
χ_f	T_t (°C) (±0.1°C)	E_a (kJ/mol)	ΔH (kJ/mol)	T_m (°C) (±0.08°C)
EtOH				
0	80.0	441 ± 29	409 ± 28	83.36
0.023	76.0	377 ± 13	302 ± _21	77.24
0.032	75.7	308 ± 25	– [a]	– [a]
0.040	72.5	249 ± 45	287 ± 20	71.80
0.049	74.1	427 ± 18	240 ± 24	74.97
D_2O				
1	84.3	482 ± 33	249 ± 19	86.33

[a] Not measured.

position into several steps can be hypothesized assuming a Lumry–Eyring-type mechanism [28]:

$$N\text{–}Cu^{2+} \overset{K}{\leftrightarrow} U \overset{k}{\rightarrow} F \qquad (b)$$

where U is the unfolded state, K is the equilibrium constant, and k is the kinetic constant.

To determine the thermodynamic and kinetic parameters of the DSC transition, the Lumry–Eyring model as modified by Sanchez–Ruiz (negligible heat exchange associated to the step $U \rightarrow F$) [29] and recently improved by Milardi et al. (not negligible enthalpy of the process $U \rightarrow F$) [23] has been applied. The four experimental $C_{p,exc}$ curves (Fig. 5B) have been fitted with the following equation:

$$C_{p,exc} = \left[\frac{K\Delta H_u}{(K+1)^2} \left(\frac{k}{v} + \frac{\Delta H_u}{RT^2} \right) + \Delta H_{ag} \frac{1}{v} \frac{kK}{K+1} \right] \times \exp\left(-\frac{1}{v} \int_{T_0}^{T} \frac{kK}{K+1} \, dT \right) \qquad (4)$$

where K is the thermodynamic equilibrium constant associated with the reversible step,

$$K = \exp\left[-\frac{\Delta H_u}{R} \left(\frac{1}{T} - \frac{1}{T_{1/2}} \right) \right] \qquad (5)$$

k is the kinetic constant of the irreversible step,

$$k = \exp\left[-\frac{E}{R} \left(\frac{1}{T} - \frac{1}{T^*} \right) \right] \qquad (6)$$

ΔH_u is the thermodynamic enthalpy associated to the $N\text{–}Cu^{2+} \leftrightarrow U$ unfolding step, E and ΔH_{ag} are the activation energy and enthalpy associated with the irreversible process respectively, $T_{1/2}$ and T^* are the temperatures at which the equilibrium constant, K, and the kinetic constant, k, approach unity, respectively. In Eq. 4, ΔH_u, ΔH_{ag}, E, $T_{1/2}$ and T^* are the unknown parameters. It should be considered that the relation between the activation energy of the irreversible step, E, and the apparent activation energy, E_{app}, obtained by means of Eq. 2, is given by the following expression [29]:

$$E_{app} = E + \Delta H_u + \Delta H_{ag} \qquad (7)$$

By fitting the calorimetric experimental curve, recorded at $v = 0.7$°C/min, with Eq. 4 the following results are obtained: $\Delta H_u = 648$ kJ/mol, $\Delta H_{ag} = -372$ kJ/mol, $E = 80$ kJ/mol, $T^* = 89$°C and $T_{1/2} = 86$°C.

The results of the fitting procedure are given in Fig. 1 (dashed line on right-hand side). As can be seen, the fit is really good. Similar analysis was also carried out for the scan rates 0.3, 0.5 and 1.0°C/min. In these cases only a slight modification of the above parameters was found, proving that the applied procedure is acceptable.

In summary, taking into account the overall results, the following path of the denaturation of azurin in aqueous solution can be proposed:

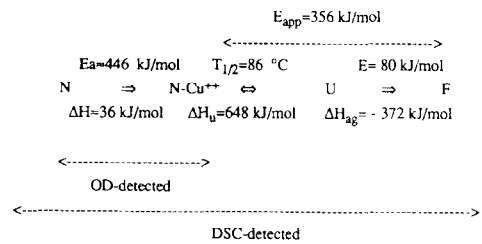

3.2. Effect of solvents on the thermal denaturation

To get more insight into the effect of solvents, the OD_{625}/T and the DSC curves of azurin in ethanol–water mixtures ($0 < \chi_f \leq 0.049$) and in D_2O (Fig. 7A and B, Table 2) have been investigated. Both profiles are very similar to those found in H_2O suggesting that the denaturation path is maintained. Moreover, azurin in D_2O shows higher T_t and T_m values than in H_2O and a lower ΔH value. The increase in T_t and T_m is ascribable to the fact that the deuteron bond D · · · OD is stronger than the corresponding H · · · OH one [30]. So the hydrophobic and hydrophilic interactions within the protein and between the protein and the solvent are stronger in D_2O than in H_2O. In the light of this fact, $\Delta H = 249$ kJ/mol found in D_2O seems quite strange. However, it must be considered that during the denaturation process the intramolecular bonds break, and the reformation of bonds between the solvent molecules and the hydrophilic and hydrophobic amino acid residues of the polypeptide chain occurs. In the enthalpic balance, bond-breaking is an endothermic

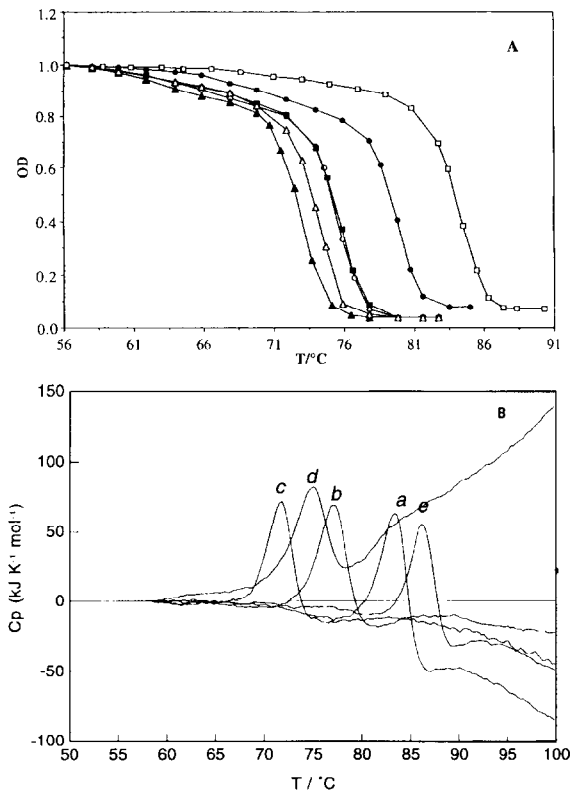

Fig. 7. (A) Normalized OD_{625} /temperature profiles obtained at a scan rate of 0.7°C/min of azurin in ethanol–water mixtures at different ethanol molar fraction: (●) $\chi_f = 0.0$; (■) $\chi_f = 0.023$; (○) $\chi_f = 0.032$; (▲) $\chi_f = 0.040$; (△) $\chi_f = 0.049$ and in (□) D_2O. (B) DSC profiles obtained at the scan rate of 0.5°C/min of azurin (1.2 mg/ml) in ethanol–water mixtures with (a) $\chi_f = 0.0$, (b) $\chi_f = 0.023$, (c) $\chi_f = 0.040$, (d) $\chi_f = 0.049$ and in (e) D_2O.

process, while bond-formation has an exothermic character. In D_2O the exothermic effect prevails.

The time-dependent OD curves were recorded at four temperatures slightly below that of the irreversible denaturation in D_2O (84.3°C). The experimental points were fitted with Eq. 1 in order to determine the kinetic rate constants, k_1. The E_a value calculated from Eq. 3 is $E_a = 482$ kJ/mol, which is higher than that determined in H_2O (441 kJ/mol). This result evidences the stabilizing role of D_2O in the irreversible alteration of the copper environment.

The optical and DSC parameters found in alcohol–water mixtures show the same trend. In fact, in the presence of ethanol T_t reduces to 76°C at $\chi_f =$ 0.023 and keeps this value up to $\chi_f = 0.032$ (Table 2). A further reduction of T_t to 72.5°C is observed at $\chi_f = 0.040$. Surprisingly, this trend reverses at $\chi_f =$ 0.049, i.e., in the presence of the highest ethanol molar fraction used.

Similarly, the DSC profiles reported in Fig. 7B show that the thermodynamic T_m value first decreases and then, at the highest ethanol concentration, increases. Only a progressive reduction of ΔH is found by increasing χ_f (Table 2). E_a related to the copper-binding-site modification (OD_{625}/time measurements) decreases up to 249 kJ/mol by increasing χ_f up to 0.040 while, at $\chi_f = 0.049$ it increases to 427 kJ/mol (Table 2).

The effect of ethanol on the thermal denaturation of azurin agrees with that reported for metal-free proteins like ribonuclease A [31,38] and lysozyme [32,33], i.e., T_t decreases with alcohol concentration. A destabilizing effect of ethanol on azurin has previously been observed by fluorescence and optical absorption measurements at room temperature [34]. These latest results explain the reduction of $\Delta T = T_m - T_t$ with the alcohol concentration.

In heme proteins [35–37], a variation of the spin state of Fe^{3+} from $S = 5/2$ to $S = 1/2$ has been observed suggesting a direct interaction of alcohol with iron in the heme pocket. In our case, however, the ethanol molecules do not directly interact with copper. The interaction is mediated by the protein surface.

Perturbation of the water layer (clathrate) around the apolar amino acid residues exposed to the solvent, decrease in the water activity with organic co-solvents, and increase in the molecular dynamics with temperature explain the phenomena observed [1,5,33,39].

At $\chi_f = 0.049$, T_t and T_m increase but not ΔH (Table 2). To understand this behavior it should be noted that: (i) at this molar fraction the thermodynamic properties of ethanol–water mixtures show a discontinuity. For example, the partial molar volume of the mixture, defined as $V_m = (\partial V_m/\partial n)_{P,T}$, decreases rapidly up to about $\chi_f = 0.049$ and then increases to the molar value of pure ethanol [40]. (ii) Ultrasound propagation measurements of ethanol–water mixtures suggest the formation of ethanol–water microstructures at $\chi_f = 0.049$, i.e., one ethanol molecule is surrounded by 17 water molecules

[41,42]. Ethanol in solution decreases the dielectric constant of the solvent, too [43]. So, that it reduces the alcohol–azurin interaction and predominates that with water and/or with other alcohol molecules. The reduced dielectric constant of the solvent makes the protein–alcohol binding sites no longer desirable for the interaction. The alcohol molecules leave the azurin–alcohol complex and the quite alcohol-free protein partially recovers its native stability.

This mechanism explains the value of the apparent activation energy as well as the increase in T_t and T_m found at $\chi_f = 0.049$ (Table 2). On the contrary, the decrease in ΔH is ascribable to the balance of the endothermic and exothermic processes involved in the denaturation.

4. Conclusion

The thermal denaturation of azurin in H_2O is a multistep irreversible, kinetically controlled process. It can be summarised as follows: as the temperature increases, azurin progresses irreversibly from the native state, N, to a folded intermediate state, N–Cu^{2+}, which involves a copper environment alteration. This step is characterised by the disappearing of the CT band at 625 nm. The ESR spectrum of this colourless form of azurin corresponds to that of a square planar Cu^{2+} complex with likely nitrogens and oxygens as ligands. The apparent activation energy, E_a, of this step has been calculated using OD_{625}/T curves obtained at different scan rates and OD_{625}/time decay profiles as well.

The DSC profile of azurin shows an endothermic and exothermic peak. The calorimetrically detected denaturation process has been decomposed in a two-step process: the first reversible, the second irreversible and under kinetic control ($N–Cu^{2+} \leftrightarrow U \rightarrow F$). This model has been tested by a curve-fitting program running with an equation which describes the $C_{p,exc}$ function in all the temperature ranges investigated. The apparent activation energy value of the denaturation of azurin on the whole was evaluated from the scan rate dependent DSC profiles.

The solvent strongly influences the thermal stability of the protein but not the denaturation path. In D_2O the steps of the denaturation process of azurin occur at temperatures higher than in H_2O. In addition, the E_a value found in D_2O by means of OD measurements is higher than in H_2O.

In ethanol–water mixtures, however, the denaturation shows a behavior which depends on the solvent composition. At lower χ_f values, all denaturation steps shift to lower temperatures, while the apparent activation energy, E_a, reduces; at $\chi_f = 0.049$ the trend reverses.

Acknowledgements

R.G. thanks the MURST for a fellowship. This work was financially supported by CNR and MURST research grants.

References

[1] J.L. Finney, B.J. Gellatly, I.C. Golton and J. Goodfellow, Biophys. J., 32 (1980) 17.
[2] G. Némethy, W.J. Peer and H.A. Scheraga, Ann. Rev. Biophys. Bioeng., 10 (1981) 459.
[3] A.J. Doig and D.H. Williams, J. Mol. Biol., 217 (1991) 389.
[4] P.L. Privalov, E.I. Tiktopulo, S.Yu. Venyaminov, Yu.V. Griko, G.I. Makhatadze and N.N. Khechinashvili, J. Mol. Biol., 205 (1989) 737.
[5] P.H. Von Hippel and K.Y. Wong, J. Biol. Chem., 240 (1963) 3909.
[6] A. Cupane, D. Giacomazza, F. Madonia, P.L. San Biagio and E. Vitrano, in A. Borsellino, P. Omodeo, R. Strom, A. Vecli and E. Wanke (Eds.), Development in Biophysical Research, New York, 1980, p. 269.
[7] A. Cupane, M. Leone, E. Vitrano and L. Cordone, Biophys. Chem., 38 (1990) 213.
[8] L. Sportelli, A. Desideri and A. Campaniello, Z. Naturforsch., 40C (1985) 551.
[9] P.L. Privalov and S.A. Potekhin, Methods Enzymol., 131 (1986) 1.
[10] R. Jaenicke, Phil. Trans. R. Soc. Lond. B, 326 (1990) 535.
[11] E.T. Adman, G.W. Canters, H.A.O. Hill and N.A. Kitchen, FEBS Lett., 143 (1982) 287.
[12] C.M. Groeneveld, M.C. Feiters, S.S.Hasnain, J. van Rijn, J. Reedijk and G.W. Canters, Biochim. Biophys. Acta, 873 (1986) 214.
[13] I.A. Fee, in: D.J. Dunitz, P. Hemmerch, R.H. Holm, J.A. Ibers, C.K. Jorgensen, J.B. Neilands, D. Reinen and R.J.P. Williams (Eds.), Structure and Bonding, Vol. 23, Springer, Berlin/Heidelbeg/New York, 1975, pp. 2–60.
[14] E.I. Solomon, J.W. Hare, D.M. Dooley, J.H. Dawson, P.J. Stephens and H.B. Gray, J. Am. Chem. Soc., 102 (1980) 168.

[15] E.G. Norris, B.F. Anderson and E.N. Baker, J. Am. Chem. Soc., 108 (1986) 2784.
[16] E.N. Baker, J. Mol. Biol., 203 (1988) 1071.
[17] H. Nar, A. Messerschmidt, R. Huber, M. van de Kamp and G.W. Canters, J. Mol. Biol., 218 (1991) 427.
[18] A. Romero, C.W.G. Hoitink, H. Nar, R. Huber, A. Messerschmidt and G.W. Canters, J. Mol. Biol., 229 (1993) 1007.
[19] A.A. Gerwith and E.I. Solomon, J. Am. Chem. Soc., 110 (1988) 3811.
[20] E.I. Solomon, M.J. Baldwin and M.D. Lowery, Chem. Rev., 92 (1992) 521.
[21] E.T. Adman and L.H. Jensen, Isr. J. Chem., 21 (1981) 8.
[22] M.L. Galisteo and J.M. Sanchez-Ruiz, Eur. Biophys. J., 22 (1993) 25.
[23] D. Milardi, C. La Rosa and D. Grasso, Biophys. Chem., 52 (1994) 183.
[24] H.E. Engeseth and D.R. McMillin, Biochemistry, 25 (1986) 2448.
[25] J. Peisach and W.E. Blumberg, Arch. Biochem. Biophys., 165 (1974) 691.
[26] T. den Blaawen and G.W. Canters, J. Am. Chem. Soc., 115 (1993) 1121.
[27] J.M. Sànchez-Ruiz, J.L. Lòpez-Lacomba, M. Cortijo and P.L. Mateo, Biochemistry, 27 (1988) 1648.
[28] R. Lumry and H. Eyring, J. Phys. Chem., 58 (1954) 110.
[29] J.M. Sànchez-Ruiz, Biophys. J., 61 (1992) 921.
[30] G. Némethy and H.A. Scheraga, J. Phys. Chem., 41 (1964) 680.
[31] R.G. Biringer and A.L. Fink, J. Mol. Biol., 160 (1982) 87.
[32] G. Velicelebi and J.M. Sturtevant, Biochemistry, 18 (1979) 1180.
[33] J.M. Sturtevant, Proc. Natl. Acad. Sci. USA, 74 (1977) 2236.
[34] R. Guzzi and L. Sportelli, J. Inorg. Biochem., 45 (1992) 39.
[35] A.S. Brill, B.W. Castleman and M.E. McKnight, Biochemistry, 15 (1976) 2309.
[36] B.B. Muhoberac and A.S. Brill, Biochemistry, 19 (1980) 5157.
[37] S. Cannistraro, Chem. Phys. Lett., 122 (1985) 165.
[38] J.F. Brandts and L. Hunt, J. Am. Chem. Soc., 89 (1967) 4826.
[39] K. Kuczera, J. Kuriyan and M. Karplus, J. Mol. Biol., 213 (1990) 351.
[40] A.K. Mishra and J.C. Ahluwalia, J. Phys. Chem., 88 (1984) 86.
[41] E.K. Baumgartner and G. Atkinson, J. Phys. Chem., 75 (1971) 2336.
[42] E.K. Baumgartner and G. Atkinson, Z. Phys. Chem., 252 (1973) 392.
[43] G. Baldini, H. Fu-Hua, G. Varani, L. Cordone, S.L. Fornili and G. Onori, Nuovo Cimento D, 6 (1985) 618.